We thank the Editor Stephen Hicks for handling our submission and two reviewers for providing very useful and constructive comments. Please find below our point-to-point replies to the comments raised by the two reviewers, together with a summary of changes made in the revised manuscript. We hope the revised manuscript will be considered suitable for publication in *Seismica*.

Black: original comments from reviewers
Blue: our replies
Purple: cited (unchanged) texts from the original manuscript
Red: changes made in the revised manuscript

Line numbers refer to the revised version under track mode, excluding those mentioned in the comments

---

Reviewer A:
This manuscript presents 2.5D dynamic rupture simulations in a splay-and-main fault system in order to understand the backward rupture branching - a feature deemed impossible before - observed during the 2023 Mw 7.8 Turkey earthquake. The manuscript is divided in two main parts, the first (short) part analyzes seismic observations to characterize the rupture path of the Turkey earthquake. The second (main) part of the paper presents the dynamic simulation results. The manuscript is well written, overall easy to follow, and nicely illustrated by high-quality figures. It is a significant and interesting contribution as it explores through a wide range of dynamic rupture simulations the different scenarios that can lead to a backward rupture branching, as well as how the initial parameters impact the branching characteristics (NE and SW time delays) and the rupture characteristics (rupture speed, slip amplitude) on both the splay and main faults. Two main mechanisms of backward branching are identified and explained through very clear figures and pertinent analyses (coulomb stress change and shear stressing rate). I have few comments, questions or suggestions, which are minor for most of them. I enjoyed reading this manuscript.
We thank the reviewer for the positive evaluation of our work.

Major comments:
1. Please discuss your results with respect to the other dynamic rupture simulation papers that have been published recently for this earthquake: Zhe et al. (2023) and Wang et al. (2023). In particular, the mechanism of backward branching illustrated in Figure 5 is the same as the one presented in Zhe et al. (2023), while the scenarios presented in Figures 8b and 8c seem more similar to the results of Wang et al. (2023). Please cite and discuss your results in light of these papers.
Thanks for mentioning other published works. We were not aware of Jia et al. (2023) and Wang et al. (2023) when working on this project. The original ideas for understanding backward branching with the same sense of shear were proposed by Fliss et al. (2005) and Oglesby et al. (2003), and were recognized by us on February 7, 2023 (https://twitter.com/XRupture/status/1622919814691045378), just one day after the occurrence of the 2023 Turkey (now renamed as Kahramanmaraş (Türkiye)) earthquake sequence. The work of Fliss et al. (2005) is more relevant to our study (2-D) and has been already cited in our original manuscript. Per the reviewer's request, we also cite and discuss Jia et al. (2023) and Wang et al. (2023) in the revised manuscript.

Lines 471-473: The above mechanism was first proposed by Fliss et al. (2005) for the 1992 M_w 7.3 Landers earthquake in California, and has also been invoked by other research groups for understanding the 2023 M_w 7.8 Kahramanmaraş earthquake in Türkiye (Jia et al., 2023; Liu et al., 2023).

Lines 563-566: First, the triggered rupture along the main fault can be asymmetric, featuring supershear towards NE but subshear towards SW (Figure 8b and c), which can still be attributed to the asymmetric ΔCFS across the junction along the main fault and has also been confirmed by 3-D numerical simulations (Wang et al., 2023).

The main differences between our study and those of Jia et al. (2023) and Wang et al. (2023) lie in dimensionality, stress/strength variation along depth, and free surface. We briefly discuss these points in section 4.1.

Lines 737-739: Similar cascade process is also seen in 3-D numerical simulations (Jia et al., 2023), with a possible preference of rupture triggering near the free surface (Wang et al., 2023).

Lines 761-763: Future studies can be conducted to explore other conditions (e.g., 3-D effects, free surface effects, gap or overlap between different fault segments) that can promote or impede backward rupture branching (Jia et al., 2023; Oglesby et al., 2003; Wang et al., 2023).

2. Figure 3 and L222-223. Most of the stations are significantly shifted from the fault, please make it clear in the text that the estimation is very rough and give at best a lower bound of the rupture speed on the SW part of the EAF. On the NE part, it seems impossible to estimate a rupture speed from the four stations available in the area. Three of them are truncated and the passage of the rupture front cannot be clearly identified in the fourth one (unlike the stations in the SW part, for which the passage of the rupture front is clear). The 3.2 km/s green dotted line should be removed from the figure.
We totally agree. Following the suggestion, we remove the dotted line marked with 3.2 km/s towards NE of the EAF, please check the revised Figure 3b. For clarity, we also add the following sentences.

Lines 261-270: Assuming that the initial rupture arrived at the junction at around 16 s, we argue that a new rupture initiated along the EAF somewhere near the junction. This new rupture showed a clear propagation phase to the SW, according to the moveouts of coherent high-frequency signals later than 20 s (indicated by the dashed green line in Figure 3b). A very rough estimation, based on the onsets of these late signals, yields a propagation speed of ~ 3.5 km/s (probably a lower bound) along the EAF west of the junction. As for the NE part of the EAF, it is difficult to track the rupture trajectory, due to the truncated waveforms at three stations. Although uncertainties still remain about the exact initiation location and earlier propagation speed of the rupture along the EAF, the strong ground motion data confirm a pattern of rupture branching from the splay fault to the EAF (at least its SW part), consistent with the back-projection results.

Lines 279-280 (caption for Figure 3): Due to the truncated waveforms at stations 0208, 4631 and 0213, the rupture trajectory in the NE direction cannot be unambiguously tracked.

3. L 344-345 and Figures 5 & 6: why did you choose to showcase this model rather than another one with successful rupture branching? If this is your preferred model, consider stating it clearly in the paper and explain why. I understand that the goal of this paper is to identify a range of possible scenarios and not to make a detailed comparison with the data, but it would still be interesting to discuss which scenario is the most probable in the case of the Turkey earthquake.
Thanks for raising this point. We show the subshear scenario (on both splay fault and main fault) in Figures 5 and 6 merely as a reference model. We had no solid observational evidence to support this scenario when preparing our initial submission. Even at the time of writing this reply, it remains debated whether the rupture reaches supershear along the splay fault (Delouis et al., 2023; Rosakis et al., 2023) or along the main fault (Jia et al., 2023; Liu et al., 2023; Wang et al., 2023). Ambiguity also exists on whether the SW segment of the EAF fails significantly later than the NE segment (Jia et al., 2023; Liu et al., 2023; see also our later replies to the 4th and 11th minor comments). More conclusive answers to the above issues may be reached by future observational studies. To avoid confusion, we add some sentences to clarify that Figures 5 and 6 serve only as a reference model, with no particular endorsement. We also mention the current disagreement in resolving rupture behaviors among different research groups.

Lines 425-427: This case is presented only for demonstrating one possible mode of the branching process; it does not necessarily represent our preferred scenario for the 2023 M_w 7.8 Kahramanmaraş earthquake.

Lines 744-755: According to our parameter space study, the second mode may seem less likely, due to the required condition of close-to-failure initial shear stress for the main fault (extremely low S^m in Figure S11). However, such condition can still be realized by localized stress concentration near a fault junction (not modeled in this study), as implied by earthquake cycle simulations (Duan and Oglesby, 2007) and the seismicity pattern before the 2023 earthquake sequence (Güvercin et al., 2022; Kwiatek et al., 2023). Therefore, the possibility for the second mode cannot be completely ruled out. From the observational point of view, while a number of research papers have now been published, it is still difficult to discern which mode is more likely to be involved during the 2023 M_w 7.8 Kahramanmaraş earthquake. For example, the work of Jia et al. (2023) favors a significantly delayed triggering (~ 10 s) of the backward (SW) segment of the EAF, while that of Liu et al. (2023) shows almost simultaneous triggering of both the backward (SW) and forward (NE) segments of the EAF. Despite a difference in the branching process, both works confirm the occurrence of backward rupture branching.

Minor comments:

(**m-1**) Title: This event is now called 'Kahramanmaraş'. Consider changing "the 2023 Mw 7.8 Turkey earthquake" to "the 2023 Mw 7.8 Kahramanmaraş, Turkey, earthquake"
We now revise the name of the earthquake as "the 2023 M_w 7.8 Kahramanmaraş (Türkiye) earthquake". We also update the official name for Turkey (now spelled as Türkiye) at various places.

(**m-2**) L. 82 "previously unmapped splay fault" Not entirely true. There were discontinuous segments already mapped at the location of the splay fault (e.g. 'Narli fault' in Emre et al., 2018)
We now revise the sentence as "The rupture started on a splay fault called Narlı fault (Barbot et al., 2023; Emre et al., 2018) …".

(**m-3**) L. 89 "Dominated by left-lateral rupture" Note that optical correlation results actually show that the splay fault has a significant normal component (Fig. 4 in Karabulut et al.,2023)
We now revise the sentence as "The overall co-seismic slip was dominated by left-lateral strike-slip with minor normal or thrust component (Karabulut et al., 2023; Liu et al., 2023), …".
By minor, we don't mean to say the dip-slip component is negligible in the absolute sense, but rather mean that the dip-slip component is smaller than the strike-slip component (as in Fig. 4 of Karabulut et al., 2023).

(**m-4**) L. 184-186: "Due to the limited resolution and possibly interference between waves from multiple rupture fronts, it is challenging to determine whether the SW-ward rupture initiated simultaneously with the NE-ward rupture or after a delay.

Kinematic slip modeling of Zhe et al (2023) shows that the fit to the on-fault strong motion stations is much better with a delay of 10 seconds for the nucleation of the SW segment than without time delay (figures 2B and S17 in Zhe et al. 2023).
We thank the reviewer for directing us to the work of Jia et al. (2023).

First of all, we kindly remind the reviewer that the statement here refers to the limitations of teleseismic back-projection (BP). Synthetic tests have shown that BP using a single array best works for a unilateral

rupture, and can lose the resolution for a bilateral rupture (e.g., Li et al., 2022). We now make this point clear in the revised version.

Lines 222-225: Due to the limited resolution and possibly interference between waves from multiple rupture fronts, it is challenging to determine whether the SW-ward rupture initiated simultaneously with the NE-ward rupture or after a delay, based on teleseismic back-projection only (Li et al., 2022).

Secondly, even considering the strong ground motion data, inverting the rupture process can still be challenging. It depends on the baseline correction of the raw data, signal-to-noise ratio, frequency range for filtering, and some inherent constraints or limitations of the inversion approach. Also note that multiple patches may be nucleated simultaneously under dynamic loading. Therefore, a lower misfit in certain model space does not necessarily mean a closer match with the truth. In fact, a recently published work by Liu et al. (2023) shows that rupture may be initiated almost simultaneously on both the NE and SW segments of the EAF. For reference, we attach their fig. 8 below: please focus on 0-10s and 10-20s intervals. 0 km for the larger rectangular box (EAF) corresponds to the fault junction intersected by the splay fault.

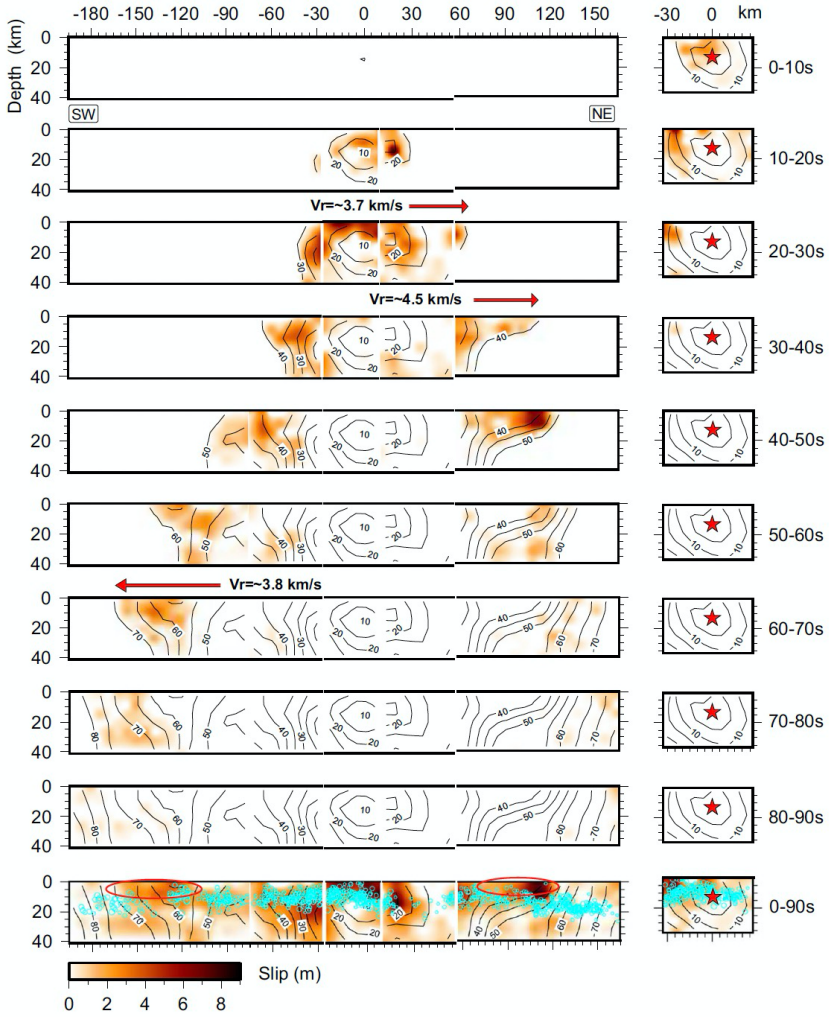

Fig. 8 | Slip time interval snapshots that highlight the supershear rupture segments for the M_W 7.8 event. The red-filled star indicates the hypocenter. Black contours represent the slip initiation time with an interval of 5 s. Cyan circles in the lower panel indicate the relocated aftershocks, with the radius scaled by magnitude. The red ovals and red arrows highlight shallow fault stretches with inferred supershear rupture, which has a notable paucity of aftershocks.

Fig. 8 from Liu et al. (2023), https://doi.org/10.1038/s41467-023-41404-5, under a Creative Commons Attribution 4.0 International License

As both Jia et al. (2023) and Liu et al. (2023) have utilized the strong ground motion data, the apparent discrepancy (whether there is a 10s delay for the SW segment of the EAF) may stem from the detailed data processing and inversion approach. It is beyond our ability to discern whose result is closer to the truth; nonetheless, we believe our original statement (lines 227-229 in the revised version) about the difficulty in resolving rupture initiation along the main fault is still valid, and we prefer to keep it.

(**m-5**) L. 296-297 & L. 364 "Due to the lack of near-field dynamic stress measurements, we cannot directly constrain f_s and f_d; we thus set their values based on trial and error"
Please consider explaining a little bit more how you chose the parameters, in particular, what lead you to choose different fs and fp values for the main and the splay faults (e.g. for the case shown in Figure 5)?
Per the request, we add the following details.

Lines 362-369: Due to the lack of near-field dynamic stress measurements, we cannot directly constrain f_s and f_d; we thus set their values based on trial and error. Specifically, we use observation-inverted fault slip (e.g., Melgar et al., 2023; Okuwaki et al., 2023) to estimate the values for stress drop and thus for f_d, while roughly guess the values for f_s based on the fault geometry and regional stress field (Figure 4). We note that, in order to rupture the misoriented splay fault ($10°$ to $\sigma^0_{\max}$), its f_s has to be somewhat lowered compared to the more optimally-oriented main fault (Fletcher et al., 2016). A new, preliminary study using in situ collected serpentine-rich rock samples shows relatively low friction of 0.28-0.55 at low slip rates (Kitajima et al., 2023), consistent with our assumed values for f_s (Table 1).

(**m-6**) L. 256: "For the Pazarcık segment, we set the angle Ψ between the maximum compressive stress σomax and the main fault at 40°." Does this value agree with Guvercin's estimation in the Pazarcik area?
Yes, the assumed angle Ψ of 40° roughly agrees with Güvercin et al.'s result for the Pazarcık segment. Note the Pazarcık segment is slightly curved, so there might be some 5° variation, depending on which side across the junction is chosen as the reference plane (Ψ is set at 44° for the Pazarcık segment in Abdelmeguid et al. (2023)). We actually referred to Güvercin et al. (2022, figs. 7 and 8) before choosing our preferred orientation for the maximum compressive stress $\sigma^0_{\max}$, as mentioned in our original text.

(**m-7**) L. 284 - 286: "Such treatment allows for through-going rupture along the main fault but terminated rupture along the splay fault (zero splay-fault slip at the junction), which is supported by the relative maturity of the main fault (the EAF) and source inversion results (Melgar et al., 2023; Okuwaki et al., 2023)." The reasoning is not very clear. Please consider clarifying your point.
We clarify the reasoning in the revised version by expanding the arguments:

Lines 342-346: Such treatment allows for through-going rupture along the main fault but terminated rupture along the splay fault (zero splay-fault slip at the junction), which is supported by the relative maturity of the main fault, making it more likely to exhibit a continuous fault geometry compared to the splay fault, and the source inversion results, in which slip at the junction tapers to zero along the splay fault but remains finite along the main fault (Melgar et al., 2023; Okuwaki et al., 2023).

(**m-8**) L. 263: "In the southward portion of the splay fault (dashed grey line in Figure 4), we assume a fault cohesion of 10 MPa to artificially terminate the rupture at around 20 km from the hypocenter." Please indicate the cohesion value on the other part of the faults (even if it is 0).
Clarified.

Lines 326-328: A fault cohesion of 10 MPa is set to terminate the southward rupture along the splay fault (dashed grey line). Elsewhere, fault cohesion is set at zero, unless mentioned otherwise.

(**m-9**) L. 405: Such asymmetric slip distribution is also observed in the case with supershear rupture along the splay fault (Figure S5), in the source inversion results for the Mw 7.8 mainshock (Barbot et al., 2023; Melgar et al., 2023; Okuwaki et al., 2023), and in other studies of the rupture branching problem (Bhat et al., 2007a; Fliss et al., 2005; Templeton et al., 2009; Xu et al., 2015), suggesting that it should be a common feature around fault junctions (Andrews, 1989)"

The asymmetric slip distribution is also observed in the static slip model and dynamic rupture model of Zhe et al. (2023) and in the dynamic rupture model of Wang et al. (2023). Please, consider citing these papers.
The two recent papers are now cited.

Lines 492-495: Such asymmetric slip distribution is also observed in the case with supershear rupture along the splay fault (Figure S6), in the kinematic or dynamic models for the M_w 7.8 mainshock (Barbot et al., 2023; Jia et al., 2023; Melgar et al., 2023; Okuwaki et al., 2023; Wang et al., 2023) …

(**m-10**) L. 486-487: Is there a particular reason why you choose to vary fs for the second set of simulations (so fs on the splay fault) while you chose to vary fd for the first set of simulations (on the main fault)?
We choose to vary fs (on the splay fault) for the second set of simulations, so that each case would produce roughly equal amounts of stress drop and slip that are consistent with observations. For the first set, we fix fs and vary fd on the main fault, so that in each case the main fault can be successfully triggered by the splay-fault rupture (as shown by the Coulomb stress change computation in Figure 5). We cite the original sentences or add new ones to explain the aforementioned reasons.

Lines 553-555 (for the first set): For the main fault, we vary f_d^m (under fixed $f_s^m = 0.48$) to obtain different values for S^m. Under this consideration, rupture can always be triggered along the main fault (at least for the NE segment), as predicted by the ΔCFS computation in Figure 5.

Lines 588-591 (for the second set): For simulating the three examples, we fix the parameters along the main fault ($f_s^m = 0.48$, $f_d^m = 0.29$, $D_c^m = 1.00$ m, $S^m = 0.73$) and some parameters along the splay fault ($f_d^{sp} = 0.10$, $D_c^{sp} = 0.50$ m).The latter choice ensures that stress drop and final slip would be roughly the same along the splay fault for all three examples.

(**m-11**) L. 534-536: "Although we do not know whether this scenario indeed occurred during the mainshock,[...]"

Please consider revising your statement. Previously published papers suggest either that the rupture propagated bilaterally once the junction was reached; or that the NE part ruptured first, and then the SW part after a delay. There is no evidence suggesting that the SW part ruptured first. So it seems that this scenario can be ruled out in the case of the Turkey earthquake. It is nonetheless worth exploring this scenario to identify all possible backward branching mechanisms in like-wise fault system configuration.
Thanks for the suggestion. After careful consideration, we decide to keep this statement for the following reasons.
(1) This reflects the fact — at the time of working on this project, which was initiated in February, 2023, we indeed did not know whether this scenario (early triggering on the SW segment) occurred. Please note the timelines: submission of our work (July 12, 2023), first release of Jia et al. (August 3, 2023), publication of Liu et al. (September 9, 2023). Earlier publications (e.g., Melgar et al., 2023; Okuwaki et al.,

2023) focus on reporting first-order features, and probably cannot provide a convincing answer to which side of the EAF ruptured first.
(2) Historic lesson from the 2011 Tohoku earthquake tells us that earlier published studies (e.g., with the maximum slip around the hypocenter) are not necessarily correct, and hence there is no reason for us to ignore other possibilities. With the release of more data and the aid of large-scale computing, researchers may finally manage to identify the most likely scenario, but this takes time.
(3) From personal communication, we learn that one observational study has found evidence for early triggering on the SW segment. Unfortunately, that study is still under review with no copies publicly available on preprint servers, so that we cannot cite or discuss it in our manuscript, at least for now.
(4) The main purpose of our work is to explore a range of possible scenarios and to provide mechanical basis for each scenario. We have already clarified that we don't aim to perform a close comparison with observations (lines 127-129 in the revised version).

To help readers understand why we explore the scenario of early triggering of the SW segment, we make the following revision.

Lines 661-662: Motivated by our previous study on backthrust fault branching (fig. 5 in Xu et al. (2015)), we also find cases in which rupture is triggered first on the SW segment of the main fault.

Figures:

- Figure 2: the scale is missing for the size-coded power of the radiators.
We now add the information of size-coded power. Please check the revised Figure 2. Note that we don't use exaggerated circle sizes, so that each high-frequency radiator can be clearly seen, without being masked by larger (more energetic) ones.

- Figure 5: please add the value of the S ratio in the legend or wihtin the main text.
Done.

- Figure 7: could you please indicate on this plot which model corresponds to the one showed in Figure 5?
We use red edge color in Figures 7, 9 and 10 to indicate the position of the reference case in Figure 5.

- Figure 10: please indicate in the legend that those quantities are measured just before the junction with the main fault (for clarity).
We add the following sentence to the caption of Figure 10.

Lines 654-655: Note that rupture speed regime and $|\dot{\tau}|$ are examined for the northward splay-fault rupture front, right before it hits the junction.

Newly cited references:

Emre, Ö., Duman, T. Y., Özalp, S., Şaroğlu, F., Olgun, Ş., Elmacı, H., and Çan, T. (2018). Active fault database of Turkey. *Bulletin of Earthquake Engineering*, 16(8), 3229–3275. doi: 10.1007/s10518-016-0041-2.

Jia, Z., Jin, Z., Marchandon, M., Ulrich, T., Gabriel, A. A., Fan, W. et al. (2023). The complex dynamics of the 2023 Kahramanmaraş, Turkey, M_w 7.8-7.7 earthquake doublet. *Science*, 381(6661), 985-990. doi: 10.1126/science.adi0685.

Karabulut, H., Güvercin, S. E., Hollingsworth, J., and Konca, A. Ö. (2023). Long silence on the East Anatolian Fault Zone (Southern Turkey) ends with devastating double earthquakes (6 February 2023) over a seismic gap: implications for the seismic potential in the Eastern Mediterranean region. *Journal of the Geological Society*, 180(3). doi: 10.1144/jgs2023-021.

Kitajima, H., Gomila, R., Tesei, T., Favero, M., Di Toro, G., Kondo, H. et al. (2023). Frictional behaviors of the serpentine-rich East Anatolian Fault Rocks collected from the 2014 Kartal trench site. Poster Presentation #112 at 2023 SCEC Annual Meeting.

Li, B., Wu, B., Bao, H., Oglesby, D. D., Ghosh, A., Gabriel, A. -A., et al. (2022). Rupture heterogeneity and directivity effects in back-projection analysis. *Journal of Geophysical Research: Solid Earth*, 127, e2021JB022663. doi: 10.1029/2021JB022663.

Liu, C., Lay, T., Wang, R., Taymaz, T., Xie, Z., Xiong, X. et al. (2023). Complex multi-fault rupture and triggering during the 2023 earthquake doublet in southeastern Türkiye. *Nature Communications*, 14, 5564. doi: 10.1038/s41467-023-41404-5.

Wang, Z., Zhang, W., Taymaz, T., He, Z., Xu, T., and Zhang, Z. (2023). Dynamic rupture process of the 2023 *Mw* 7.8 Kahramanmaraş earthquake (SE Türkiye): Variable rupture speed and implications for seismic hazard. *Geophysical Research Letters*, 50, e2023GL104787. doi: 10.1029/2023GL104787.

Reviewer B:

Review of Ding et al., 2023

I enjoyed reading the manuscript “The sharp turn: backward rupture branching during the 2023 Mw 7.8 Turkey earthquake,” by Ding et al. The authors utilize the aftershock catalog, teleseismic back-projection, and strong ground motion recordings to argue that in this event, rupture nucleated on a small splay fault to the south of the main East Anatolian Fault (EAF), then propagated bilaterally on this larger fault. Importantly, this rupture propagation pattern includes “backwards branching” via an acute angle between the splay and the southwestern segment of the EAF. This behavior has been considered unlikely or even prohibited by stress shadowing in simple dynamic models of branch fault systems, so the authors then carry out a series of 2.5D dynamic models to investigate the circumstances under which such branching behavior may take place. They find that such propagation is indeed possible under different combinations of fault stress and frictional parameters, through one of two mechanisms: First, rupture propagates to the end of the splay, and then initially toward the more favored northeast segment of the EAF, followed by delayed propagation to the southwest EAF. Second: rupture propagates rapidly to the southwest EAF before rupture reaching the end of the splay in highly-prestressed cases.

As the authors note, their model is not designed to be a comprehensive simulation of the 2023 M7.8 event; their fault geometry, material structure, and other parameters are all quite simplified from the real world. Rather, they endeavor to conduct an in-depth parameter study of the branching behavior by itself, and examine how it depends on a number of different physical parameters. I very much like models like this. Although modern modeling methods can do a remarkable job of incorporating wide ranges of complexity and producing physically realistic results, there is still quite an important role for simple parameter studies: they can give insight into physical mechanisms that could be obscured in a tremendously complex model, and thus (in my opinion) may have more predictive power for future

earthquakes in other settings. I find the methods sound and the results quite reasonable. My comments are overall quite minor, and I believe that this manuscript will be suitable for publication with minor revisions. My detailed line-by-line comments are below.
We thank the reviewer for the positive evaluation of our work. We are delighted to know that the reviewer also appreciates the power of simple models (more outcomes than inputs).

1. 17: It would be good to specify the lines of evidence by name in this introductory sentence.
We revise the opening statement of the abstract to make the message more explicit.

Lines 26-28: Surface rupture trace, earthquake relocation, teleseismic and strong ground motion observations, and published source inversion studies indicate that the 2023 M_w 7.8 Kahramanmaraş (Türkiye) earthquake started on a splay fault …

2. Figure 1: You might want to comment on the fact that your modeled splay fault is consistent with the aftershock distribution on the splay, even though it is longer than the mapped surface trace of the splay.
We clarify in the caption of Figure 1 that our simplified fault geometry for the splay fault is consistent with aftershock distribution.

Lines 167-168: For the splay fault that hosted the hypocenter of the M_w 7.8 event, the modeled fault is longer than the mapped surface rupture trace, but is consistent with the aftershock distribution.

3. 220 – 222: It's not clear to me how you read a rupture speed from the East data; I don't see any particular arrival at the estimated time at station 4611. It's more convincing for the West stations.
We apologize for the inconvenience. It is indeed impossible to read the rupture speed in the NE direction. Now we remove the dashed green dashed line marked with 3.2 km/s in Figure 3b. We also add the following sentences to clarify the situation.

Lines 266-270: As for the NE part of the EAF, it is difficult to track the rupture trajectory, due to the truncated waveforms at three stations. Although uncertainties still remain about the exact initiation location and earlier propagation speed of the rupture along the EAF, the strong ground motion data confirm a pattern of rupture branching from the splay fault to the EAF (at least its SW part), consistent with the back-projection results.

Lines 279-280: Due to the truncated waveforms at stations 0208, 4631 and 0213, the rupture trajectory in the NE direction cannot be unambiguously tracked.

4. 308-309: This is a very interesting physical point. Did the authors document this result enough to document it--perhaps in the supplementary materials if it's outside the main scope of the paper? They show the effect of Dc later, but don't show models that die out, I believe.
For completeness, we have tried even larger Dc values (e.g., 4 m and 8 m) during our initial numerical tests, and found that no rupture continuation could exist under such conditions. As observations show successful triggering and continued rupture on both NE and SW segments of the EAF, we mainly focus on showing numerical results with triggered and sustained ruptures.

Lines 380-381: Larger D_c values (e.g., $\geq$ 4.0 m) in general do not favor successful rupture branching and hence can be readily ruled out.

Lines 555-556 (caption for Figure 7): For clarity, results are shown for triggered ruptures that can continue to propagate along the main fault.

5. 328-329: Can you elaborate a bit on how this W factor is implemented in your 2D code?, and what effects it has on the results?
A more complete description of the 2.5-D model (history, implementation) can be found in Weng and Ampuero (2019, 2020). In the revised version, we briefly mention the implementation of the W factor in the 2-D code and its effects.

Lines 401-405: A parameter W is introduced to mimic the fault width, which modifies the original 2-D equation of momentum balance by taking into account the traction applied at the top or bottom boundary of the seismogenic zone. Such modification causes a saturation of slip and stress intensity factor, associated to a transition from crack-like to pulse-like rupture, once the along-strike propagation distance exceeds a value proportional to W (Day, 1982).

6. 384-386: It would be helpful to put one of those models with the NE main fault blocked off in the supplementary materials. It is a very important point the authors are making here, with potential significant impact on rupture path estimates worldwide.
We add two new figures (Figures S4 and S8) in the supplementary material: one shows failed triggering of the SW main fault if the NE main fault is blocked off (Figure S4), the other shows early and successful triggering of the SW main fault even without the NE main fault (Figure S8). Due to the inclusion of these two new figures, we also update the figure number in the supplementary material.

7. 392-395: Does this rupture behavior agree with that inferred from data?
As said in our replies to the first reviewer, the current observational studies have not yet reached an overall agreement on the detailed branching process, e.g., whether there is a significant delay for the rupture triggering on the SW segment of the main fault. In the result section (Section 3), we prefer to focus on presenting our simulation results. In the discussion (Section 4.1), we briefly mention the results of some observational studies.

Lines 743-755: In both modes, successful backward rupture branching can be realized for a range of rupture speeds along the splay fault (Figures 9 and S11). According to our parameter space study, the second mode may seem less likely, due to the required condition of close-to-failure initial shear stress for the main fault (extremely low S^m in Figure S11). However, such condition can still be realized by localized stress concentration near a fault junction (not modeled in this study), as implied by earthquake cycle simulations (Duan and Oglesby, 2007) and the seismicity pattern before the 2023 earthquake sequence (Güvercin et al., 2022; Kwiatek et al., 2023). Therefore, the possibility for the second mode cannot be completely ruled out. From the observational point of view, while a number of research papers have now been published, it is still difficult to discern which mode is more likely to be involved during the 2023 M_w 7.8 Kahramanmaraş earthquake. For example, the work of Jia et al. (2023) favors a significantly delayed triggering (~ 10 s) of the backward (SW) segment of the EAF, while that of Liu et al. (2023) shows almost simultaneous triggering of both the backward (SW) and forward (NE) segments of the EAF. Despite a difference in the branching process, both works confirm the occurrence of backward rupture branching.

8. Figure 7 (and similar figures later): I found the color scale on this figure to be a bit confusing. The colorbar implies (at least to me) that there is a continuous range of Dcm, while in fact there are 4 discrete sets of models with 4 different values of Dcm. I suggest the authors label the colors differently, without a colorbar.
We now change the way of showing Dc values to reflect their discrete nature. Please check the revised Figures 7, 9 and 10.

9. Figure 8 (some thoughts on the physical mechanism): The supershear rupture on the splay fault could break up rupture directivity; perhaps the higher directivity effect in the subshear splay facilitates rapid transition to supershear on the NE main fault. Furthermore, for a while after the supershear transition on the splay, the energy release on the splay is partitioned between 2 pulses (the daughter and parent cracks), which means that there is less energy release in either individual crack.
We thank the reviewer for providing additional insights into the triggering process. We revise the sentence to include the suggested mechanism.

Lines 601-605: First, $|\dot{\tau}|$ for a splay-fault subshear rupture is higher than that for a splay-fault supershear rupture (Figure 10d and e), at least for the cases investigated in this study. This can be attributed to the higher degree of stress singularity in the subshear regime (Freund, 1990), and possibly also to the enhanced effects of directivity and energy release for a subshear rupture (the corresponding effects could be reduced for a supershear rupture where energy is partitioned between the leading and trailing fronts).

10. Caption to figure 8: It would help to mention the S values on the splay as well as its frictional coefficients.
We add the information of the S values to the caption of Figure 8.

Lines 591-593: We vary the static friction coefficient along the splay fault to obtain different S ratios and to produce different rupture behaviors: (a) $f_s^{sp} = 0.21$, $S^{sp} = 0.08$; (b) $f_s^{sp} = 0.25$, $S^{sp} = 0.47$; (c) $f_s^{sp} = 0.33$, $S^{sp} = 1.26$.

11. 541-546: I'm a little unclear on the point of this section. Don't the data imply a delay, making the idea of accelerated triggering of the SW segment a contrary-to-observation exercise? There's nothing wrong with such exercises because they can lead to increased physical insight, but they should be clearly indicated.
The investigation of this early-triggering mode was motivated by our previous study (Xu et al., 2015), which shows that backward fault segment may be first triggered before the preceding rupture reaches the fault junction. In fact, we had little knowledge about the actual branching process when preparing this manuscript, which also explains why we decided to explore a range of possible scenarios. Even for now, we still don't know whether the activation of the SW segment of EAF is significantly delayed (see our reply to comment 7, as well as replies to the first reviewer). Therefore, we don't think the idea of early triggering of the SW segment necessarily conflicts with observation; instead, it can motivate observational seismologists to refine the analysis of available data, and to connect pre-earthquake stress state with foreshock activity and co-seismic rupture behavior. To clarify, we add some sentences in the revised version.

Lines 661-664: Motivated by our previous study on backthrust fault branching (fig. 5 in Xu et al. (2015)), we also find cases in which rupture is triggered first on the SW segment of the main fault. Although we do not know whether this scenario indeed occurred during the mainshock, it is interesting to explore its features for the following three reasons.

Lines 750-755: From the observational point of view, while a number of research papers have now been published, it is still difficult to discern which mode is more likely to be involved during the 2023 M_w 7.8 Kahramanmaraş earthquake. For example, the work of Jia et al. (2023) favors a significantly delayed triggering (~ 10 s) of the backward (SW) segment of the EAF, while that of Liu et al. (2023) shows almost simultaneous triggering of both the backward (SW) and forward (NE) segments of the EAF. Despite a difference in the branching process, both works confirm the occurrence of backward rupture branching.

Other changes made during revision

Title: The sharp turn: Backward rupture branching during the 2023 M_w 7.8 Kahramanmaraş (Türkiye) earthquake

Figure 11 has been updated, to correct for a display error for V_P' and V_S'.

Figures 4, 6, 11, S4, S6, S8, and S10 have been updated, to correct for a slightly display error for the north direction indicator to better match the fault geometry identified from Figure 1.

Lines 841-850: Back-propagating rupture has been reported in slow earthquakes (Houston et al., 2011; Obara et al., 2012), regular earthquakes (Hicks et al., 2020; Ide et al., 2011; Meng et al., 2012b) and laboratory earthquakes (Gvirtzman and Fineberg, 2021; Xu et al., 2023; Yamashita et al., 2022). Multiple mechanisms have been proposed to explain its occurrence: stress transfer along a heterogeneous fault (Luo and Ampuero, 2017), pore-pressure wave (Cruz-Atienza et al., 2018), low-velocity fault damage zone (Idini and Ampuero, 2020), free-surface reflection (Oglesby et al., 1998), coalescence of two rupture fronts (Yamashita et al., 2022).

We update the formatting for displaying figure captions.

We also update the reference list.